


Nonisothermal crystallization kinetics of bio-based semi-aromatic polyamides

Xueke Sun¹  · Kancheng Mai¹ · Chuanhui Zhang² · Min Cao² · Yingying Zhang³ · Xinghong Zhang³

Received: 14 October 2016 / Accepted: 27 April 2017 / Published online: 8 May 2017
© Akadémiai Kiadó, Budapest, Hungary 2017

Abstract Semi-aromatic copolyamides PA10T10I and PA10T10F based on bio-based poly(decamethylene terephthalamide) (PA10T) were synthesized by a two-step polycondensation technique. The nonisothermal crystallization of these semi-aromatic polyamides was investigated by differential scanning calorimetry. Avrami theory modified by Jeziorny and Mo equation was used to describe the nonisothermal crystallization kinetics of these semi-aromatic polyamides, respectively. The crystallization activation energies were obtained by Kissinger method. The crystallization temperature, crystallization rate and activation energy were explained by regularity and flexibility of chain.

Keywords Nonisothermal crystallization kinetics · Bio-based · Semi-aromatic polyamides · Poly(decamethylene terephthalamide)

Electronic supplementary material The online version of this article (doi:10.1007/s10973-017-6434-x) contains supplementary material, which is available to authorized users.

✉ Xueke Sun
sunxueke@kingfa.com.cn

- ¹ Material Science Institute, Key Laboratory of Polymeric Composites and Functional Materials of Ministry of Education, Guangdong Provincial Key Laboratory of High Performance Polymer-based Composites, Materials, School of Chemistry, Sun Yat-sen University, Guangzhou 510275, China
- ² National-certified Enterprise Technology Center, Kingfa Science and Technology Co., LTD., Guangzhou 510663, China
- ³ MOE Key Laboratory of Macromolecular Synthesis and Functionalization, Department of Polymer Science and Engineering, Zhejiang University, Hangzhou 310027, China

Introduction

Polyamides (nylons) are important commercial engineering thermo-plastics with many merits and widely applied in many fields [1, 2]. In order to meet the higher performance requirements of electronic/electric, automotive, aerospace and military industries, semi-aromatic polyamides prepared from aliphatic diamines and aromatic diacids with higher heat resistance were developed in recent years [3]. Compared with common aliphatic polyamides such as PA6 [4] and PA66 [5], semi-aromatic polyamides generally have higher use temperature, better chemical resistance, and lower moisture absorption, thus having better dimensional stability under moist conditions [3, 6].

Poly(decamethylene terephthalamide) (PA10T) is one of the commercially available semi-aromatic polyamides which was synthesized from *p*-phthalic acid (PTA) and decamethylenediamine (DA10) [7–9]. PA10T has a much higher heat resistance than aliphatic polyamides and has the lowest moisture absorption among all commercial polyamides, including aliphatic polyamides and other semi-aromatic polyamides such as PA6T and PA9T, because the longer-chain aliphatic diamines bring out much lower concentration of amide groups [10, 11]. Recently, as a bio-based polyamide synthesized by the diamine monomer DA10 from the renewable resource of castor oil, PA10T has been getting more and more attention [3, 12, 13]. Another bio-based dicarboxylic acid, 2,5-furandicarboxylic acid (FDCA), generated from fructose and galactose was reported to be used for polyester and polyamide syntheses [14–17]. However, bio-based polymers synthesized by FDCA used as the main dicarboxylic acid result in a relatively lower heat resistance, limiting the application of the resultant polymers.

It is well known that the crystallization process of a polymer dramatically affects its processing and mechanical properties through the crystal structure and morphology. In order to approach the optimum condition in an industrial process, such as extrusion, injection molding, film production, and to obtain products with better properties, it is necessary to estimate the rate of crystallization in the nonisothermal process [18]. So the investigation of polymer crystallization kinetics is significant both from the scientific and the practical perspectives [3, 19].

In this study, the samples of PA10T and two semi-aromatic copolyamides (PA10T10I, PA10T10F) based on PA10T were prepared by a two-step polycondensation technique. The nonisothermal crystallization kinetics of the aforementioned semi-aromatic polyamides was investigated by differential scanning calorimetry (DSC). Several kinetics methods were applied to analyze its crystallization process. Furthermore, the crystallization kinetics parameters and the activation energies of nonisothermal crystallization were also determined.

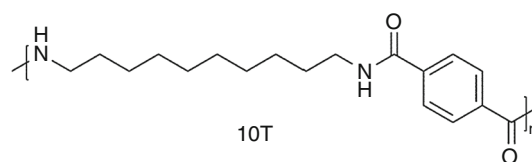
Experimental

Materials

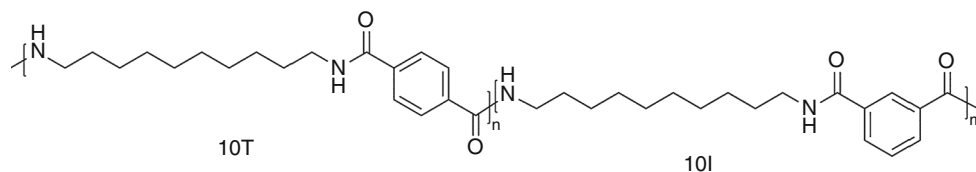
1,10-Diaminodecane ($\geq 99\%$) was purchased from Wuxi Yinda Nylon Co., Ltd. *P*-phthalic acid (PTA, $\geq 99.9\%$) was purchased from BP. 2,5-Furandicarboxylic acid (CP) was purchased from Ningbo Biomass & Biotechnology Co., Ltd. Iso-phthalic acid ($\geq 99.9\%$), benzoic acid (AR), sodium hypophosphite (AR) were purchased from

Preparation of PA10T, PA10T10I and PA10T10F

PA10T: 2960 g *p*-phthalic acid (PTA), 3200 g 1,10-Diaminodecane (DA10), 82.8 g benzoic acid, 6.2 g sodium hypophosphite and 2550 g deionized water were charged into a 20 L autoclave. Then the autoclave purged with nitrogen at 1 bar for 10 min was started to heat and stirred at 50 rpm. The temperature reached to 235 °C after about 3 h and held at this temperature for another 40 min. About 1650 g of water was discharged by a reflux condenser after about 1 h. Then the product was flushed into a nozzle open and was further dried at temperature of 100 °C to obtain a prepolymer. After prepolymerization, 5 kg of prepolymer in a 20-l vacuum tumbler was heated up to 250 °C in the 5 h, and the tumbler was kept rotating in 10 rpm at the vacuum degree of 20 Pa. During the postpolymerization process, the sample taken in an interval time of 40 min was used to measure the relative viscosity (RV). Once RV of tested sample reached the desired value, the vacuum was replaced by nitrogen, and meanwhile cooling program was began. The chemical structure of prepared PA10T repeating units determined by ^1H NMR and ^{13}C NMR is presented as follow:

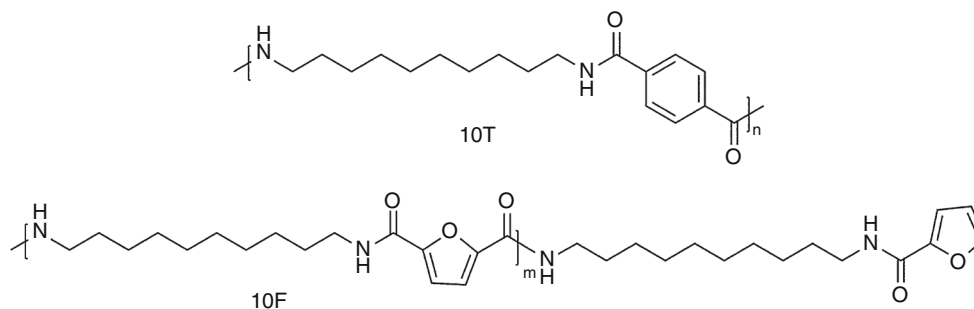


The preparation of PA10T10I was similar to PA10T except that 10% of PTA was replaced by *i*-phthalic acid (ITA). The chemical structure of its repeating units determined by ^1H NMR and ^{13}C NMR is as follow:



Guangzhou Chemical Reagent Factory. Hexafluoroisopropanol (HFIP), trifluoroacetic acid-d (CF_3COOD) concentrated sulfuric acid (96%) and Chloroform-d (CDCl_3) were purchased from J&K Chemicals.

The preparation of PA10T10F was similar to PA10T except that 30% of PTA was replaced by 2,5-furandicarboxylic acid (FDCA), and no benzoic acid was used. The chemical structure of its repeating units determined by ^1H NMR and ^{13}C NMR is as follow:



Characterization

Fourier-transform Infrared (FT-IR) spectra were obtained by using a Bruker Vector 22 FT-IR spectrophotometer (KBr disk). ^1H NMR and ^{13}C NMR spectra of the products were recorded on a Bruker Advance DMX 500-MHz spectrometer. Chemical shift values were referenced to TMS (tetramethyl silane) as internal standard at 0.0 ppm.

Relative viscosity

The proper amount of 98% sulfuric acid was placed with a pipette into a volumetric flask, after which 0.25 g sample was added. Then, the flask was put in a shaking table with water bath of 50 °C for about 1 h until the sample was dissolved completely. The flask was put in a constant temperature bath and allowed to reach 25 °C. Then, the sulfuric acid solution was diluted to 25 mL and dumped into an Ostwald viscometer. The time required for the upper meniscus to successively pass the two calibration marks of this instrument was recorded as t_1 , and the efflux time of pure sulfuric acid was recorded as t_0 . Then relative viscosity can be calculated as: $\text{RV} = t_1/t_0$. Relative viscosities of PA10T, PA10T10I, PA10T10F are 2.11, 2.04 and 1.95, respectively.

Differential scanning calorimetry

Nonisothermal crystallization kinetics were studied using a Netzsch-DSC 200 F3 differential scanning calorimeter. All DSC measurements were performed under a nitrogen atmosphere, and sample mass varied from 6 to 8 mg. Nonisothermal crystallization and melting process for PA10T, PA10T10I and PA10T10F were performed as follows: the samples were heated from room temperature to 350 °C at 20 °C min^{-1} , maintained at the same temperature for 5 min to eliminate residual crystals; then, the melt was cooled to 50 °C to crystallize at different cooling rates 2.5, 5, 10, 15, and 20 °C min^{-1} . The exothermic curves of heat flow as functions of temperature were recorded and investigated.

Polarizing optical microscopy

The crystallization morphologies of samples were observed with the polarized optical microscope ECLIPSE E600 W, which equipped with a heating and cooling stage (ED600). The nonisothermal crystallization samples were prepared after heated to 350 °C for 5 min and cooled to 100 °C at a rate of 2.5, 5, 10, 15, and 20 °C min^{-1} , respectively.

Results and discussion

Nonisothermal crystallization behaviors of PA10T, PA10T10I and PA10T10F

The nonisothermal crystallization exothermic curves of PA10T, PA10T10I and PA10T10F at various cooling rates (Φ) are shown in Fig. 1, and the related data are listed in Table 1. The crystallization peak temperature (T_p) shifts to a lower temperature region with increasing the cooling rate, while the crystallization enthalpies (ΔH_c) increased gradually. Moreover, when the cooling rate increased, the shapes of the crystallization peak become wider gradually. This is a common phenomenon for nonisothermal crystallization of semi-crystalline polymer [2, 20]. At the same cooling rate, the T_p values of PA10T were higher than those of the PA10T10I and PA10T10F. It indicated that the incorporation of 10I and 10F units into PA10T main chains resulted in the difficulty to crystallization due to the destroyed molecular chain regularity of PA10T. The T_p of PA10T10I higher than PA10T10F was attributed to the higher chain regularity.

Nonisothermal crystallization kinetics

The relative degree of crystallinity $X(T)$, at temperature T , was calculated according to the following equation:

$$X(T) = \frac{\int_{T_0}^T \frac{dH_c}{dT} dT}{\int_{T_0}^{T_\infty} \frac{dH_c}{dT} dT} \quad (1)$$

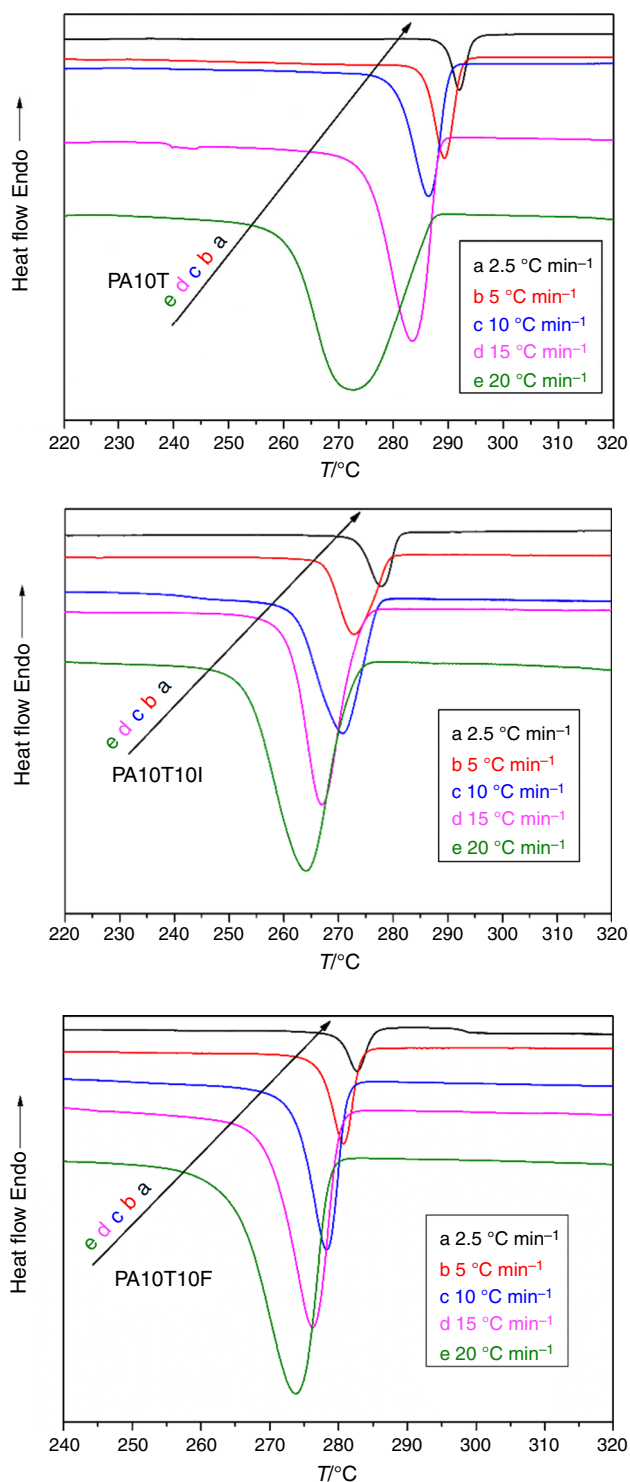


Fig. 1 DSC heat flow versus temperature during nonisothermal crystallization of PA10T, PA10T10I and PA10T10F at different cooling rates

Table 1 The DSC data of three semi-aromatic polyamides crystallized at different cooling rates

Sample	$\Phi/^\circ\text{C min}^{-1}$	$T_p/^\circ\text{C}$	$\Delta H_c/\text{J g}^{-1}$
PA10T	2.5	292.0	29.19
	5	289.2	35.60
	10	286.3	33.20
	15	283.3	48.02
	20	272.7	57.73
PA10T10I	2.5	277.9	42.49
	5	272.9	44.35
	10	270.8	46.66
	15	270.7	40.03
	20	264.0	47.71
PA10T10F	2.5	282.6	29.58
	5	280.7	37.12
	10	278.2	40.31
	15	276.3	45.14
	20	273.8	49.82

where T_0 and T_∞ are the onset and end temperatures of crystallization, respectively, and H_c is the enthalpy of crystallization.

On the basis of DSC results, the plots of the relative crystallinity $X(T)$ of PA10T, PA10T10I and PA10T10F at different crystallization temperature are shown in Fig. 2. According to the relationship of the crystallization temperature (T) and the crystallization time (t), t can be calculated by the following equation:

$$t = \frac{|T_0 - T|}{\Phi} \quad (2)$$

Plotting $X(t)$ of PA10T, PA10T10I and PA10T10F versus the crystallization time (t) at various cooling rates, S-like curves are obtained (seen in Fig. 3).

Analysis Based on the Jeziorny method

A variety of the theories developed by Avrami, Ozawa, Jeziorny, Mo et al. are often used to analyze the non-isothermal crystallization kinetics of polymers [21, 22]. For isothermal crystallization, the primary stage of crystallization is usually described by the Avrami equation [23].

$$1 - X(t) = \exp(-Kt^n) \quad (3)$$

$$\lg[-\ln(1 - X(t))] = n \lg t + \lg K \quad (4)$$

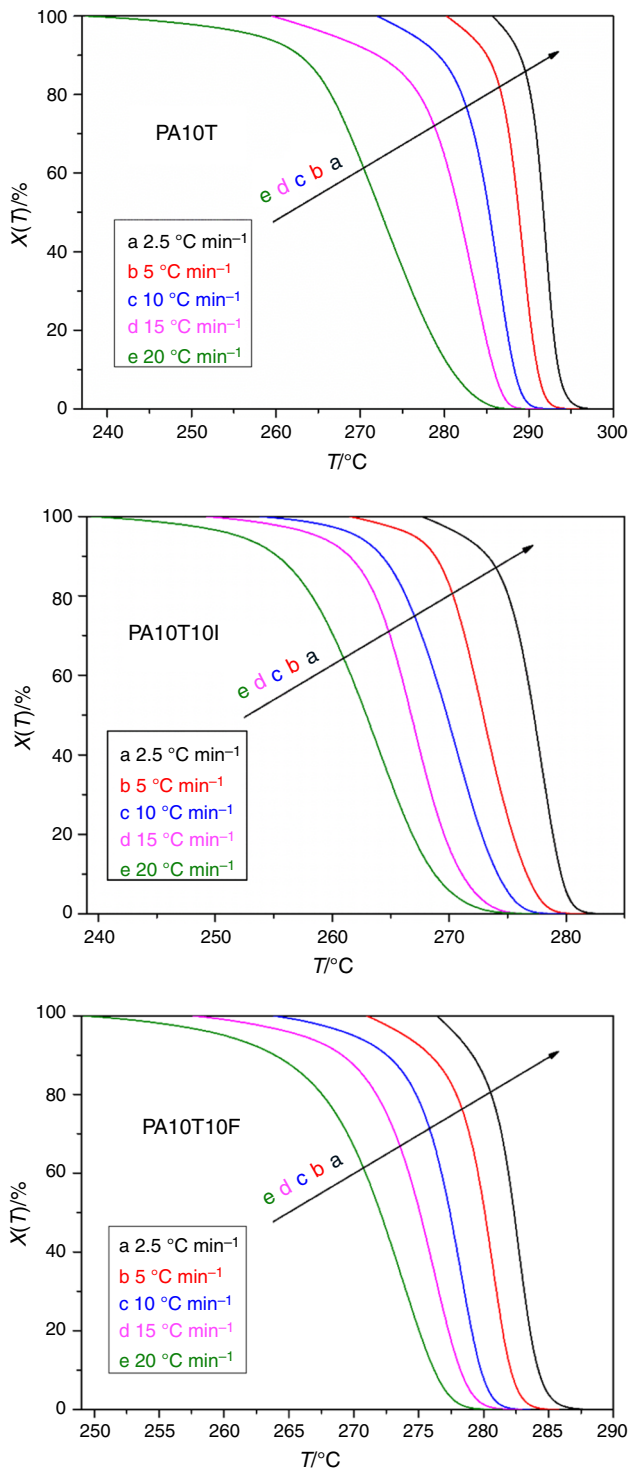


Fig. 2 Relative crystallinity $X(T)$ of PA10T, PA10T10I and PA10T10F at different crystallization temperatures in the process of nonisothermal crystallization

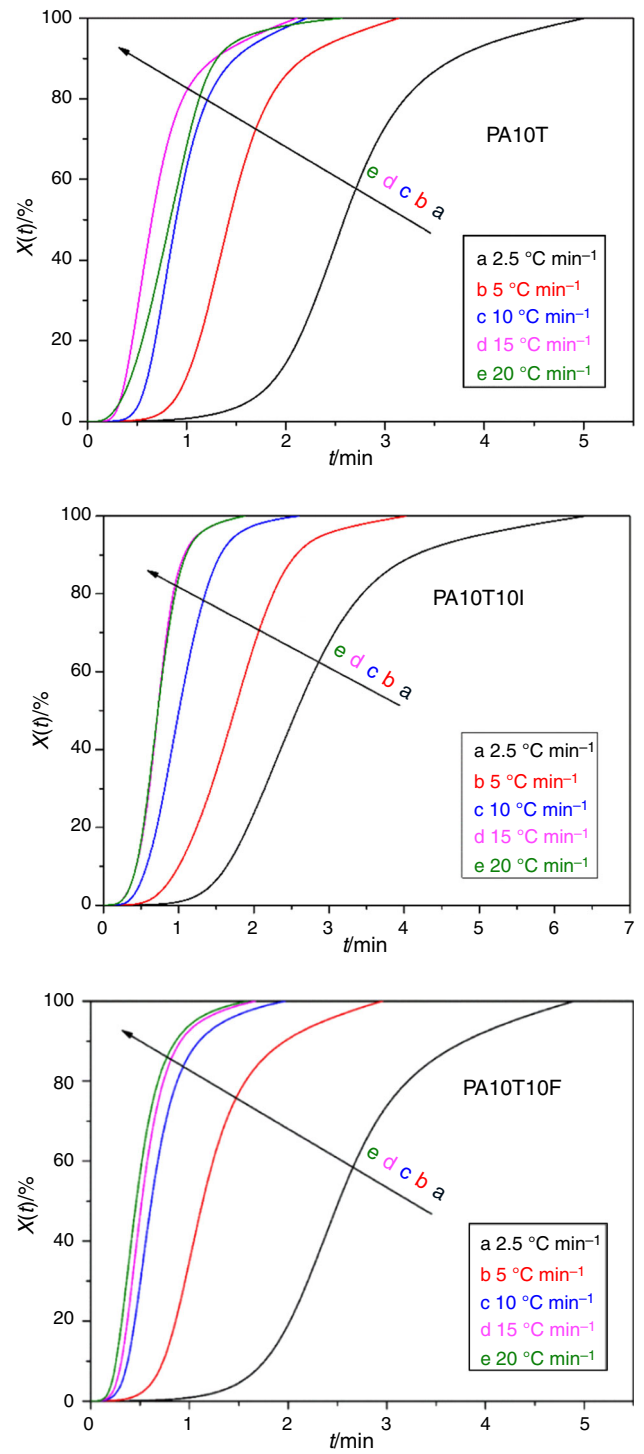


Fig. 3 Relative crystallinity $X(t)$ of PA10T, PA10T10I and PA10T10F at different crystallization times in the process of nonisothermal crystallization

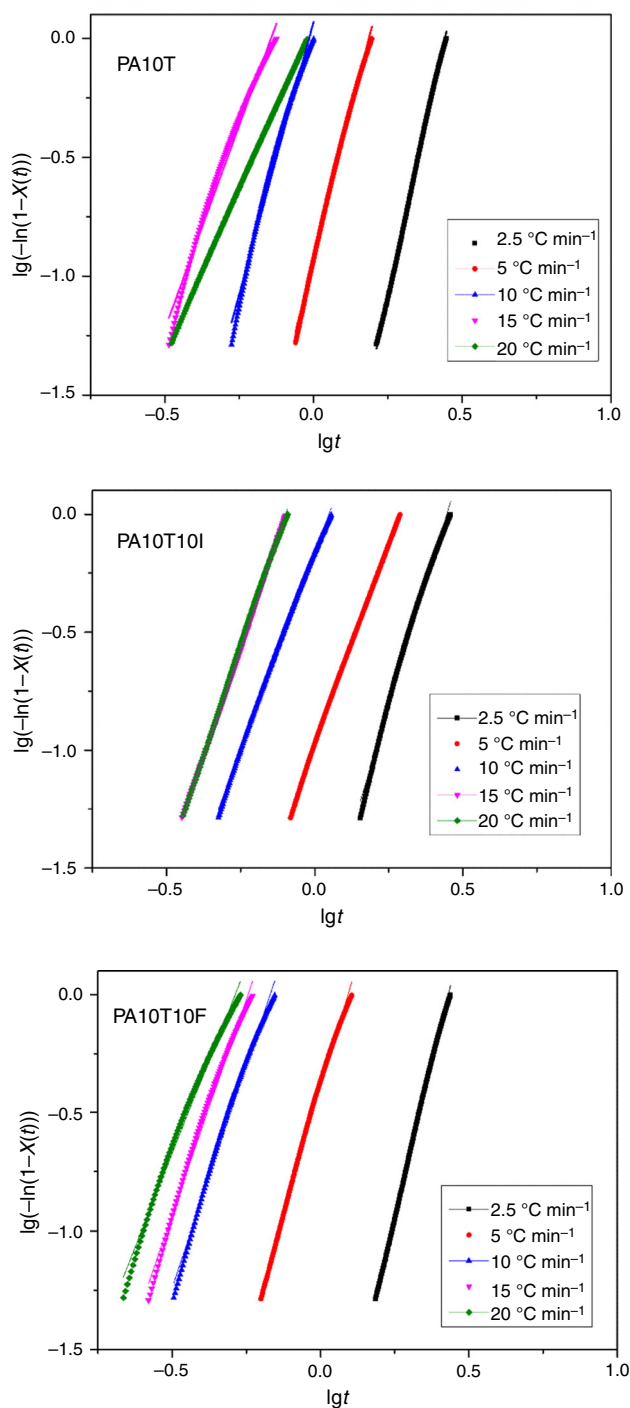


Fig. 4 Plots of $\lg[-\ln(1-X(t))]$ versus $\lg t$ for the PA10T, PA10T10I and PA10T10F

Table 2 Values of n , R^2 , K_c , $t_{1/2}$ and G at Various Cooling Rates for PA10T, PA10T10I and PA10T10F

Sample	$\Phi/^\circ\text{C min}^{-1}$	n	R^2	K_c	$t_{1/2}/\text{min}$	G/min^{-1}
PA10T	2.5	5.69	0.9993	0.10	2.59	0.39
	5	5.00	0.9962	0.65	1.50	0.66
	10	4.59	0.9887	1.02	0.90	1.11
	15	3.43	0.9880	1.08	0.65	1.54
	20	2.79	0.9998	1.01	0.84	1.19
PA10T10I	2.5	4.17	0.9931	0.18	2.57	0.39
	5	3.41	0.9994	0.64	1.74	0.57
	10	3.35	0.9987	0.96	1.01	0.99
	15	3.70	0.9997	1.06	0.72	1.39
	20	3.68	0.9994	1.04	0.72	1.39
PA10T10F	2.5	5.23	0.9988	0.13	2.51	0.40
	5	4.26	0.9956	0.83	1.14	0.88
	10	3.76	0.9933	1.16	0.62	1.61
	15	3.65	0.9927	1.15	0.52	1.92
	20	3.17	0.9913	1.11	0.46	2.17

$X(t)$ is the relative degree of crystallinity, and n is the Avrami exponent dependent on the mechanism of nucleation and the form of crystal growth, and K is the crystallization rate constant involving both nucleation and growth rate parameters.

For the nonisothermal crystallization, the K should be corrected as follows:

$$\lg K_c = \frac{\lg K}{\phi} \quad (5)$$

where K_c is the corrected crystallization rate constant of the nonisothermal crystallization by Jeziorny's theory [24].

Figure 4 shows the plots of $\lg[-\ln(1-X(t))]$ versus $\lg t$ for the PA10T, PA10T10I and PA10T10F. The parameters of the nonisothermal crystallization kinetics at the main crystallization period are shown in Table 2, and R^2 is the factors of goodness of fit of linear of regression. As seen in Table 2, the value of n at various cooling rates was in the range of 2.8–5.7 for the PA10T, PA10T10I and PA10T10F. At lower cooling rates (at 2.5, 5, 10, and 15 $^\circ\text{C min}^{-1}$), the corrected crystallization rate parameter K_c of these bio-based semi-aromatic polyamides increased

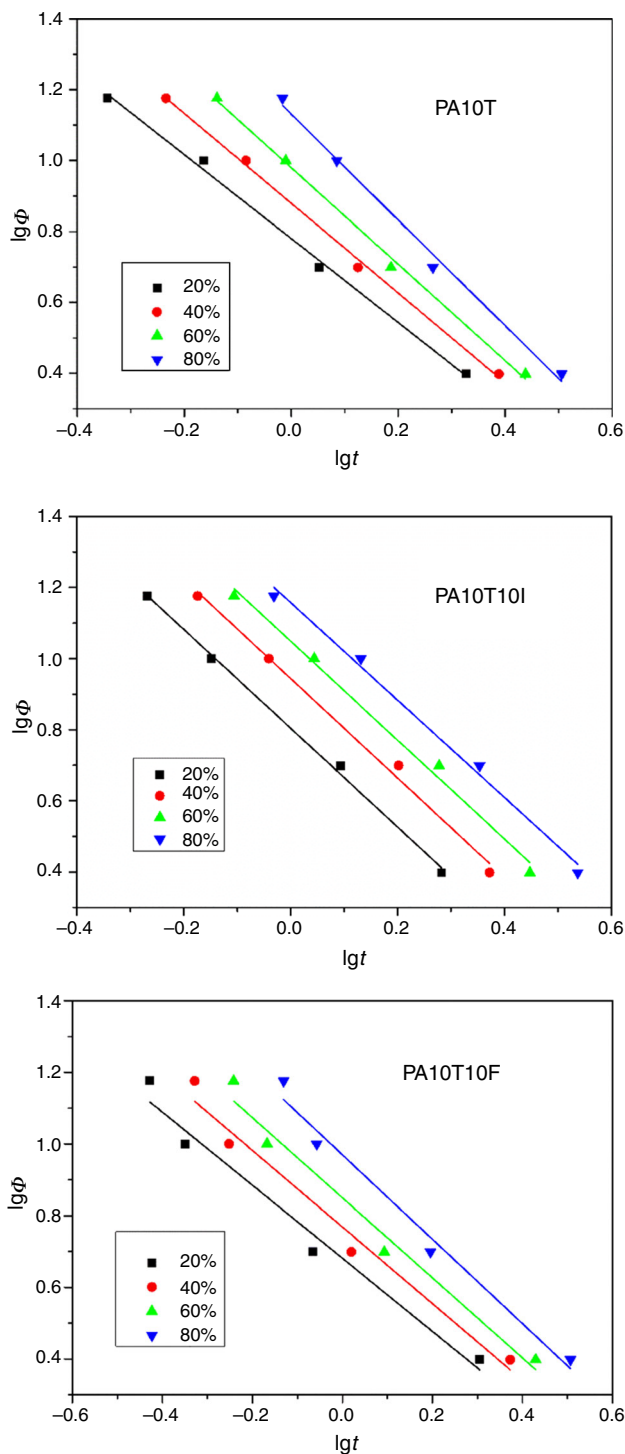


Fig. 5 The Mo plots of $\lg \Phi$ versus $\lg t$ for PA10T, PA10T10I and PA10T10F

significantly with increasing cooling rate, suggesting that the crystallization rate increased as the cooling rate increased [2]. However, at higher cooling rates (at $20\text{ }^\circ\text{C min}^{-1}$), the values of K_c were slightly decreased in comparison with the values of K_c calculated at the cooling rates of $15\text{ }^\circ\text{C min}^{-1}$, which was similar with the crystallization behavior of nylon 6 [28]. Furthermore, the sample PA10T10F always has the highest K_c value, which indicated that PA10T10F has the highest crystallization rate, while PA10T and PA10T10I have the similar crystallization rate which is much lower than PA10T10F. Besides, the crystallization rates G ($G = 1/t_{1/2}$) calculated by half time of crystallization ($t_{1/2}$) of all samples also confirmed the highest crystallization rate of PA10T10F and PA10T had a lowest crystallization rate at the same cooling rate. The results could be explained by the fact that the difference of the chain flexibility of three samples, that is, the chain units of 10I and 10F in the samples of PA10T10I and PA10T10F were more flexible than that of the chain units of 10T due to the respective incorporation of ITA and FDA moieties.

Analysis based on Mo method

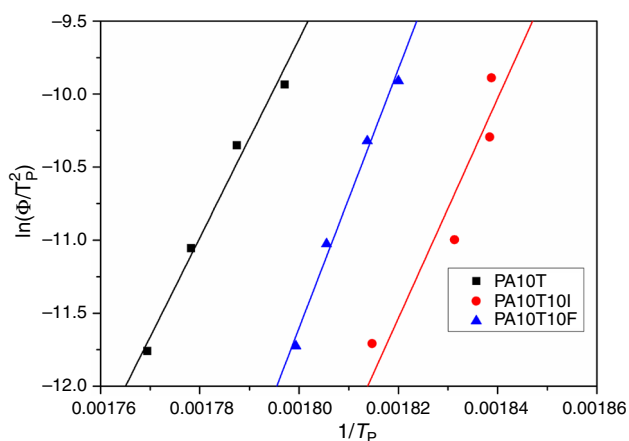
As Jeziorny’s theory is only suitable for the main crystallization period at nonisothermal crystallization conditions, Mo and coworkers combined the Avrami equation with the Ozawa equation and developed a new theory to describe exactly the nonisothermal crystallization process. Thus, a new equation is described as follows [25, 26]:

$$\lg \Phi = \lg F(T) - \alpha \lg t \tag{6}$$

where α is the ratio between the Avrami and Ozawa exponents when the system has a certain degree of crystallinity, and the parameter $F(T)$ refers to the value of cooling rate chosen at unit crystallization time [26–28]. That is, the bigger the value of $F(T)$, the slower the crystallization rate. At a given degree of crystallinity, the Mo plots of $\lg \Phi$ versus $\lg t$ for the PA10T, PA10T10I and PA10T10F are presented in Fig. 5 and the values of α , R^2 and $F(T)$ are listed in Table 3. The good linearity of the plots verifies the successful application of the combined approach in this case. As shown in Table 3, the value of $F(T)$ increased with increasing relative degree of crystallinity $X(t)$, which means that at unit crystallization time, a higher cooling rate should be adopted to obtain a higher

Table 3 The Values of $F(T)$, R^2 , and α from Mo plots for PA10T, PA10T10I and PA10T10F

Sample	PA10T			PA10T10I			PA10T10F		
	α	$F(T)$	R^2	α	$F(T)$	R^2	α	$F(T)$	R^2
20	1.18	0.78	0.9947	1.39	0.80	0.9961	1.02	0.68	0.9656
40	1.27	0.88	0.9966	1.40	0.94	0.9906	1.07	0.77	0.9667
60	1.36	0.98	0.9956	1.39	1.05	0.9884	1.12	0.85	0.9682
80	1.49	1.13	0.9903	1.37	1.16	0.9900	1.18	0.97	0.9729

**Fig. 6** The Kissinger plots of $\ln(\phi/T_p^2)$ versus $1/T_p$ for PA10T, PA10T10I and PA10T10F**Table 4** The values of ΔE and R^2 for PA10T, PA10T10I and PA10T10F

Sample	PA10T	PA10T10I	PA10T10F
$\Delta E/\text{kJ mol}^{-1}$	-564.90	-625.08	-737.06
R^2	0.9740	0.8426	0.9827

degree of crystallinity. Moreover, the crystallization rate decreased with the increase of relative degree of crystallinity at nonisothermal crystallization conditions. Table 3 shows that the values of $F(T)$ and α for the PA10T are larger than that of PA10T10F and the values of $F(T)$ and α for PA10T10I are largest among these three bio-based semi-aromatic polyamides. Mo method indicated that the values of $F(T)$ for the PA10T10F are the smallest, meaning that it has the fastest crystallization rate, as shown in the previous results.

Crystallization activation energy

Considering the influence of different cooling rate in the nonisothermal crystallization process, Kissinger suggested that crystallization activation energy (ΔE) for nonisothermal crystallization can be derived from the combination of cooling rate and crystallization peak temperature [29]:

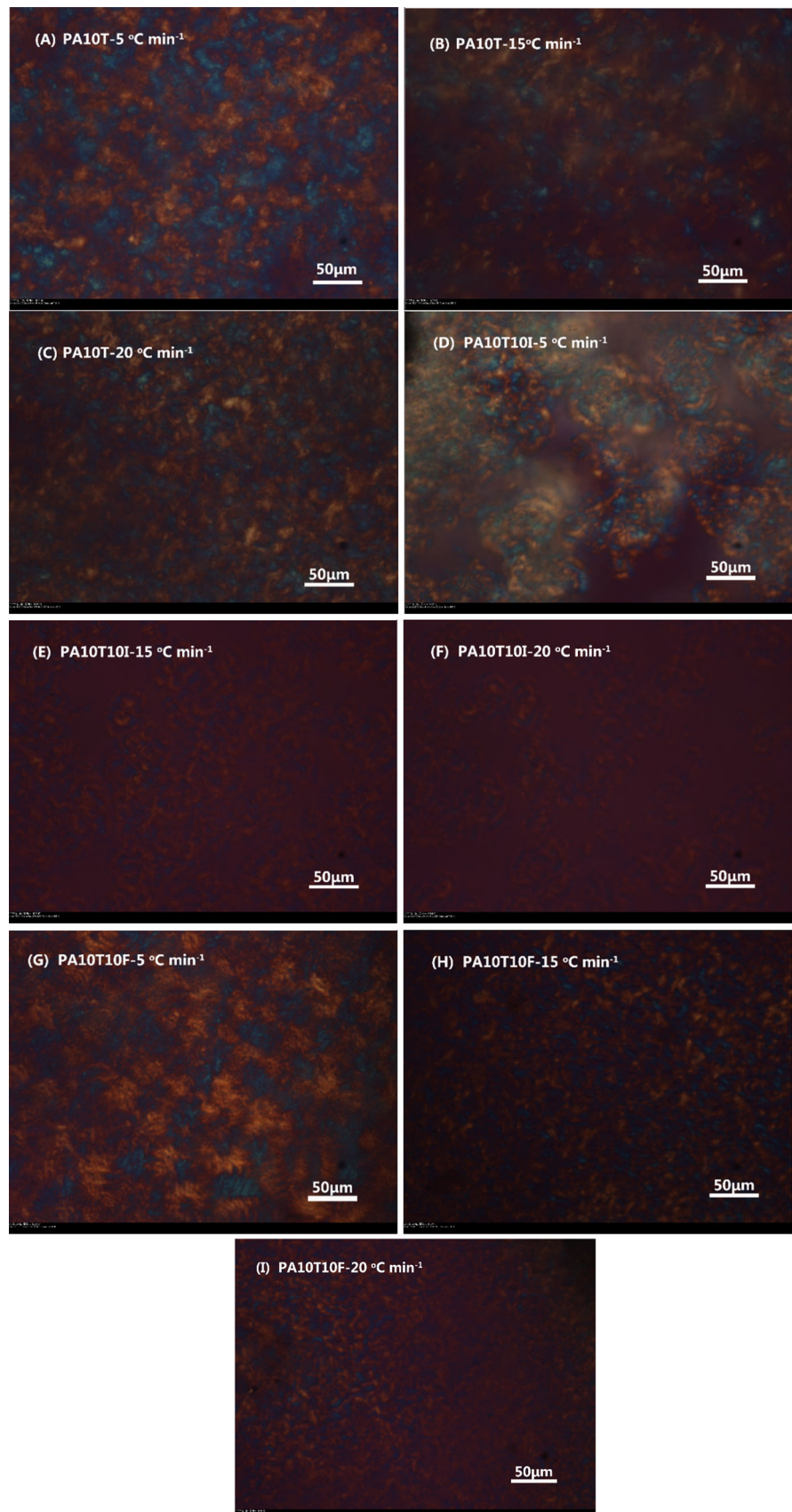
$$\frac{d[\ln(\phi/T_p^2)]}{d(1/T_p)} = -\frac{\Delta E}{R} \quad (7)$$

where R is the gas constant; T_p is the crystallization peak temperature, and ΔE is the activation energy of nonisothermal crystallization. Generally, the ΔE consists of the transport activation energy ΔE^* and the nucleation activation energy ΔF^* . ΔE^* is the free energy of activation for transporting the molecular segments across the phase boundary to the crystallization phase. ΔF^* refers to the free energy of formation of the critical size crystallization nuclei [30]. Figure 6 shows the plots of $\ln(\phi/T_p^2)$ versus $1/T_p$ for PA10T, PA10T10I and PA10T10F. From the slopes of the fitted lines, the values of ΔE and R^2 were obtained and summarized in Table 4. It can be seen that the crystallization activation energy of PA10T, PA10T10I and PA10T10F was calculated to be -564.90 , -625.08 and -737.06 kJ mol^{-1} , respectively. That is, PA10T10F presented the lowest ΔE value than the other two samples due to its more flexible chain.

Nonisothermal crystalline morphologies of PA10T, PA10T10I and PA10T10F

The polarizing micrographs of PA10T, PA10T10I and PA10T10F crystallized under different cooling rates are shown in Fig. 7. It can be seen that the size of spherulites of these three bio-based semi-aromatic polyamides decreased with increasing cooling rates. Particularly at lower cooling rates the polyamides crystallize effectively from the melt, the growing front of the spherulites overlap each other. For example, the growth of spherulites of

Fig. 7 Polarizing micrographs of PA10T, PA10T10I and PA10T10F at different cooling rates



PA10T10I observed at different cooling rates with increasing time is seen in the supporting information (Fig. S5–S9). Obviously, the spherulite size during cooling increases gradually with increasing time.

Conclusions

In this paper, we synthesized semi-aromatic copolyamides PA10T10I and PA10T10F based on bio-based poly(decamethylene terephthalamide) by a two-step polycondensation technique. The results of differential scanning calorimetry on the nonisothermal crystallization of these semi-aromatic polyamides indicated that PA10T10F exhibited higher crystallization temperature and crystallization rate than PA10T and PA10T10I. Avrami theory modified by Jeziorny and Mo equation could describe the nonisothermal crystallization kinetics of these semi-aromatic polyamides, respectively. PA10T10F has the higher crystallization rate than PA10T and PA10T10I. The crystallization activation energies calculated by Kissinger method indicated that PA10T10F has the lower crystallization activation energy. The higher crystallization temperature and crystallization rate and lower crystallization activation energy of PA10T10F were attributed to the flexibility of chain.

Acknowledgements We are grateful for the financial support from National Key Technology Support Program of the People's Republic of China (2013BAE02B00).

References

- Zhang Z, Huang K, Liu Z. Synthesis of high molecular weight nylon 46 in supercritical carbon dioxide. *Macromolecules*. 2011;44:820–5.
- Sun Z, Wang X, Guo F, Jiang C, Pan Q. Isothermal and non-isothermal crystallization kinetics of bio-sourced nylon 69. *Chin J Chem Eng*. 2016;24:638–45.
- Liu H, Yang G, He A, Wu M. Isothermal and nonisothermal crystallization kinetics of a semicrystalline copolyterephthalamide based on poly(decamethylene terephthalamide). *J Appl Polym Sci*. 2004;94:819–26.
- Millot C, Fillot L-A, Lame O, Sotta P, Seguela R. Assessment of polyamide-6 crystallinity by DSC. *J Therm Anal Calorim*. 2015;122(1):307–14.
- Layachi A, Frihi D, Satha H, Seguela R, Gherib S. Non-isothermal crystallization kinetics of polyamide 66/glass fibers/carbon black composites. *J Therm Anal Calorim*. 2016;124(3):1319–29.
- Leboeuf C. US5981692A, 1999.
- Davis AC, Edwards TE. Brit. Pat. 1070416, 1967.
- Liedloff HJ, Schmid, M. U.S. Pat. 5,708,125, 1998.
- Ng H. U.S. Pat. 6,355,769, 2002.
- Sawada M, Ogo Y. JP2002293926A, 2002.
- Nakajima M, Sekine H, Demura S. JP2002293928A, 2002.
- Kabasci S. *Polyamides from biomass derived monomers*. Hoboken: Wiley; 2013.
- Pagacz J, Raftopoulos KN, Leszczyńska A, Pieliowski K. *Bio-polyamides based on renewable raw materials*. *J Therm Anal Calorim*. 2016;123:1225–37.
- Sheldon RA. Green and sustainable manufacture of chemicals from biomass: state of the art. *Green Chem*. 2014;16:950–63.
- Gandini A. Furans as offspring of sugars and polysaccharides and progenitors of a family of remarkable polymers: a review of recent progress. *Polym Chem*. 2009;1:245–51.
- Gandini A, Lacerda TM. From monomers to polymers from renewable resources: recent advances. *Prog Polym Sci*. 2015;48:1–39.
- Sousa AF, Vilela C, Fonseca AC, Matos M, Freire CSR, Gruter GJM, Coelho JFJ, Silvestre AJD. Biobased polyesters and other polymers from 2,5-furandicarboxylic acid: a tribute to furan excellency. *Polym Chem*. 2015;6:5961–83.
- Layachi A, Frihi D, Satha H, Seguela R, Gherib S. Non-isothermal crystallization kinetics of polyamide 66/glass fibers/carbon black composites. *J Therm Anal Calorim*. 2016;3:1–11.
- Zhang Z, Chen C, Wang C, Guo J, Mai K. Nonisothermal crystallization kinetics of isotactic polypropylene nucleated with a novel supported β -nucleating agent. *J Therm Anal Calorim*. 2011;103:311–8.
- Zhang F, Wang B, Man R, Peng Z. Isothermal crystallization kinetics of in situ Nylon 6/graphene composites by differential scanning calorimetry. *Polym Eng Sci*. 2014;54:1381–8.
- Ozawa T. Kinetics of non-isothermal crystallization. *Polymer*. 1971;12:150–8.
- Fan Q, Duan F, Tian H. Non-isothermal crystallization kinetics of polypropylene and hyperbranched polyester blends. *Chin J Chem Eng*. 2015;23:441–5.
- Mandelkern L. *Methods of experimental physics*. New York: Academic Press; 1980. p. 81–105.
- Jeziorny A. Parameters characterizing the kinetics of the non-isothermal crystallization of poly(ethylene terephthalate) determined by DSC. *Polymer*. 1978;19:1142–4.
- Cui X, Qing S, Yan D. Isothermal and nonisothermal crystallization kinetics of novel odd-odd polyamide 9 11. *Eur Polym J*. 2005;41:3060–8.
- Song J, Zhang H, Ren M, Chen Q, Sun X, Wang S, Zhang H, Mo Z. Crystal transition of nylon-12,12 under drawing and annealing. *Macromol Rapid Commun*. 2005;26:487–90.
- Lorenzo MLD, Silvestre C. Non-isothermal crystallization of polymers. *Prog Polym Sci*. 1999;24:917–50.
- Zhang F, Peng XC, Yan WB, Peng ZY, Shen YQ. Nonisothermal crystallization kinetics of in situ nylon 6/graphene composites by differential scanning calorimetry. *J Polym Sci, Part B: Polym Phys*. 2011;49:1381–8.
- Kissinger HE. Variation of Peak Temperature with heating rate in differential thermal analysis. *J. Res Natl Stand*. 1956;57:217–21.
- Albano C, Papa J, Ichazo M, González J, Ustariz C. Application of different macrokinetic models to the isothermal crystallization of PP/talc blends. *Compos Struct*. 2003;62:291–302.